Catena 234 (2024) 107581

Contents lists available at ScienceDirect

Catena

journal homepage: www.elsevier.com/locate/catena

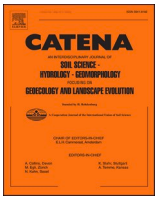

Assessing landscape ecological vulnerability to riverbank erosion in the Middle Brahmaputra floodplains of Assam, India using machine learning algorithms

Nirsobha Bhuyan [a], Haroon Sajjad [a,*], Tamal Kanti Saha [a], Roshani [a], Yatendra Sharma [a], Md Masroor [a], Md Hibjur Rahaman [a], Raihan Ahmed [b]

[a] Department of Geography, Faculty of Natural Sciences, Jamia Millia Islamia, New Delhi 110025, India
[b] Department of Geography, Nowgong College, Nagaon, Assam 782001, India

ARTICLE INFO

Keywords:
Riverbank erosion
Landscape ecological vulnerability
Artificial neural network- multilayer perceptron
Random forest
Middle Brahmaputra floodplains

ABSTRACT

Riverbank erosion is one of the most catastrophic hazards that renders floodplains vulnerable across the world vulnerable. It creates a significant negative impact on the environment and socio-economic life. This paper attempts to assess the landscape ecological vulnerability (LEV) to riverbank erosion in the Middle Brahmaputra floodplains of Assam, India by employing two machine learning models, namely artificial neural network-multilayer perceptron (ANN-MLP) and random forest (RF). Bagging ensembles were created for both ANN-MLP and RF (B-MLP and B-RF) to generate LEV zones. A total of eleven site-specific parameters were considered for the study. The receiver operating characteristic (ROC) based area under curve (AUC), accuracy, precision, recall and F1-score were used to validate the models and judge the models' performance. A sensitivity analysis was performed to deduce the most influential LEV parameters. The results revealed that B-MLP was the better-performing model compared to B-RF based on all five validation metrics. The largest area was found under very high vulnerability zone followed by very low, low, high and moderate vulnerability zones, based on both ensemble models. The western part of the floodplains was found to be more vulnerable than the eastern part. Moreover, the southern bank faced more vulnerability in comparison to the northern bank. The factors namely rainfall, soil type, vegetation and land /use land cover (LULC) influenced bank erosion vulnerability. This research provides evidence that the study area is under severe threat to riverbank erosion and urgently requires the implementation of effective mitigation measures. The study might benefit policymakers and local stakeholders to protect the floodplains from bank erosion and reduce vulnerability.

1. Introduction

Riverbank erosion is a hydrological hazard which has created severe ecological and socio-economic implications for centuries (Das et al., 2014). It is caused when the basal sediments of the banks are removed due to the hydraulic pressure exerted by the river and the nature of the bank composition (Ghosh & Sahu, 2018). Factors such as river discharge, the quantity of sediment, stream slope, the velocity of the river and the presence of vegetation regulate the process of riverbank erosion (Ahmed et al., 2018). Climate change, anthropogenic activities and the growth of population have further increased the impact of riverbank erosion in the floodplains. Rivers erode their banks laterally in the middle and lower courses due to a decrease in river velocity and gradient (Dey & Mandal, 2019). The process of lateral erosion is predominantly observed in floodplains having low-lying flat surfaces which are composed of easily erodible sediments. Floodplains are inhabited by millions of people due to the suitable topography for habitation and the availability of fertile soils for agriculture. Though they are also rich in biodiversity and maintain numerous ecosystem services, still they face the threat of erosion by rivers and are regarded as one of the most vulnerable landscapes to riverbank erosion (Hazarika et al., 2015).

Riverbank erosion has led to drastic changes in the ecology of

* Corresponding author.
E-mail addresses: nirsobhabhuyan08@gmail.com (N. Bhuyan), haroon.geog@gmail.com, hsajjad@jmi.ac.in (H. Sajjad), tamalkantisaha999@gmail.com (T. Kanti Saha), roshnisingh1405@gmail.com (Roshani), syaten25@gmail.com (Y. Sharma), mdmasroor1994@gmail.com (M. Masroor), hibjuronline@gmail.com (M.H. Rahaman), raihan.geog@gmail.com (R. Ahmed).

https://doi.org/10.1016/j.catena.2023.107581
Received 6 June 2023; Received in revised form 3 October 2023; Accepted 4 October 2023
Available online 9 October 2023

landscapes. It has affected land use/land cover (LULC) across the world (Freihardt & Frey, 2023). This was evident from the migration of the rivers in the Southern Pannonian Basin wherein cultivable land, vegetation, gravel excavations and depots, pastures and meadows were lost to bank erosion (Dragicevic et al., 2013). Along the Topl'a River in Slovakia, erosion of large areas of arable land, shrubs, forests, pastures and grasslands altered the landscape ecology and also caused substantial economic losses (Rusnák et al., 2016). The migration of the Kolubara River eroded many parcels of agricultural land and radically changed the LULC scenario of the basin it drained (Dragicevic et al., 2017; Roksandic et al., 2011). The river Nile has washed away agricultural lands through lateral erosion which in turn reduced the agricultural production of the area (Ahmed & Fawzi, 2011). The Torsa River heavily eroded the Duar and Tal regions along the Himalayan foothills leading to modifications in LULC (Dey & Mandal, 2019). Channel shifting has resulted in a decrease in the area under sparse vegetation in Murshidabad, West Bengal from 1990 to 2010 (Ghosh & Sahu, 2019). Similarly, negative change was observed for vegetation along the Padma and Mahananda rivers due to riverbank erosion from 1973 to 2016 and 1991 to 2019 respectively (Arefin et al., 2021; Chakraborty and Saha, 2021). Bhunia et al. (2016) considered bank erosion as a major driving force which has altered the LULC dynamics along the Ganges in Bihar. Debnath et al. (2017) found that the Khowai River in Tripura eroded considerable areas of agricultural land and reduced the swamps which disturbed the ecology of the area. Similar erosion of croplands and consequent creation of sandbars was noticed along the Ganga and Balasan rivers in West Bengal (Biswas & Anwaruzzaman, 2019; Das et al., 2021). Reduction in vegetal cover and wetlands was also reported in the Lower Ganga Plain due to the erosion caused by the Bhagirathi River (Paul & Bhattacharji, 2022). Riparian vegetation and floral species were drastically reduced in the São Francisco River Basin in Brazil due to riverbank erosion (Holanda et al., 2005). Negative impacts on flora, fauna and fisheries were also identified in Harirampur, Bangladesh wherein the quantity of fish harvest dwindled at a speedy rate (Bhuiyan et al., 2017).

The LULC along the Brahmaputra River also experienced changes. The area under natural grasslands and forests has decreased because of an increase in population and loss of land to riverbank erosion (Saikia et al., 2019). Pathan et al. (2021) arrived at similar conclusions regarding LULC changes in Majuli which recorded a reduction in forested lands and an increase in barren areas between 1973 and 2019. Riverbank erosion also rendered the wetlands, biodiversity and the socio-cultural foundations of the riverine island vulnerable (Sarkar, 2017; Sarma, 2014). Riparian erosion has created an imbalance in the ecosystem by endangering aquatic life and avian habitats. Bank erosion has destroyed forests which encompassed wildlife habitats and animal corridors (Dutta & Chakraborty, 2013). The erosion of lands by the Brahmaputra River forced people to illegally occupy protected forests causing deforestation and environmental deterioration (Das et al., 2014). Bank line shifting of the Subansiri, a tributary of the Brahmaputra in Assam, eroded large proportions of forested lands, bamboo cultivation and swampy areas and altered the environmental equilibrium of the area (Guite & Bora, 2016).

Landscape ecology is conceptualized as the pattern and interaction among and between different ecosystems and their impacts on ecological functions (Clark, 2010). It is a relatively new concept which emerged during the late 20th century in North America and Eastern and Central Europe (Simmons, 2004). It is a modern scientific outlook that is applicable to a wide array of ecological and social studies (Wu, 2019). Burel et al. (2013), Pearson (2020) and Kremsa (2021) equated landscape ecology with agriculture. Pearson (2013) showed the association of landscape ecology with population dynamics. The ecosystems are largely impacted by various ecological hazards (Walz et al., 2021). Several studies have been conducted to assess ecological vulnerability to different hazards. Roshani et al. (2022a), Roshani et al. (2022b) worked on inherent forest vulnerability in Darjeeling, West Bengal using the analytical hierarchy process (AHP) method. Flood susceptibility mapping was done by Hammami et al. (2019) for Tunis by applying AHP. AHP was also used by many other researchers to analyse vulnerability to various disasters (Chen et al., 2021; Mallick et al., 2018; Mondal et al., 2021; Rakotoarison et al., 2021; Tempa, 2022). In recent years, machine learning techniques have assumed great importance in vulnerability and risk assessment studies. Machine learning algorithms were applied for evaluating vulnerability to various disasters like droughts, landslides and cyclones (Azarafza et al., 2021; Hussain et al., 2022; Saha et al., 2021a, Saha et al., 2021b; Saha et al., 2023; Szczyrba et al., 2021). Deroliya et al. (2022) used decision tree (DT), random forest (RF), and gradient-boosted decision trees (GBDT) for studying flood susceptibility in the lower Mahanadi Basin in India. Bagging ensemble (BE), logistic model tree (LT), kernel support vector machine (k-SVM), and k-nearest neighbour (KNN) were applied by Al-Areeq et al. (2022) for flood zonation mapping in Jeddah, Saudi Arabia. Likewise, vulnerability to urban flash floods was examined using machine learning algorithms namely Bayesian logistic regression (BLR), artificial neural networks (ANN) and deep learning neural networks (DLNN) for Warsaw, Poland (Parvin et al., 2022). Though a large body of research on landscape ecology and ecological vulnerability has been conducted, landscape ecological vulnerability (LEV) is less explored. Some studies on landscape ecological risk assessment have been carried out (Ai et al., 2022; Gao & Song, 2022; Liu et al., 2020; Yan et al., 2021; Zhang et al., 2013). However, LEV to disasters, particularly riverbank erosion, is scarce in the existing literature. Yu et al. (2022) conducted an LEV study in the Three-River-Source National Park Region (TNPR) to analyse the spatio-temporal evolution of TNPR's LEV and the parameters influencing it.

The present study makes an attempt to assess LEV to riverbank erosion in the Middle Brahmaputra floodplains of Assam in India. The ecological vulnerability assessment is in its embryonic stage and needs further exploration. Thus, this paper aims to bridge this research gap by assessing LEV to riverbank erosion by evaluating the impact of various parameters on bank erosion vulnerability. The use of machine learning techniques has gained significant momentum, especially during the past few years for being accurate and efficient. This study makes use of two machine learning algorithms, artificial neural network-multilayer perceptron (ANN-MLP) and random forest (RF) for assessing LEV to riverbank erosion. Various scholars have utilized machine learning algorithms on ecological modelling for hazards like drought, flood and landslides (Ado et al., 2022; Masroor et al., 2023; Saha et al., 2021a, Saha et al., 2021b). These studies have found machine learning algorithms as one of the most reliable methods for relevant evaluation. However, literature on landscape ecological vulnerability to riverbank erosion using machine learning is scant. Thus, we explored the effectiveness of MLP and RF algorithms for analyzing landscape ecological vulnerability. These models are widely used for ecological modelling (Park & Lek, 2016; Shichkin et al., 2018). Further, bagging ensembles were developed for ANN-MLP and RF (B-MLP and B-RF) to prepare LEV zones. The ensemble models have advantages over single models and yield higher accuracy (Ado et al., 2022). The results of the receiver operating characteristic (ROC) curve, accuracy, precision, recall and F1-score revealed high levels of accuracy for both models. The ensemble models may be utilized for ecological modelling for similar research domains.

2. Study area

The Middle Brahmaputra floodplains in Assam spread over an area of 7294.85 km^2. It is located between 26°11′3″ N and 26°58′24″ N latitudes and 91°52′14″ E and 93°53′16″ E longitudes (Fig. 1). It is drained by one of the largest rivers in the world, the Brahmaputra River, which originates in the Kailash ranges of the Himalayas in Tibet at a height of 5300 m above sea level (Water Resources, 2023). The Brahmaputra River carries a huge amount of silt and forms an extensive braiding pattern when it enters the plains. The Brahmaputra meanders its way through

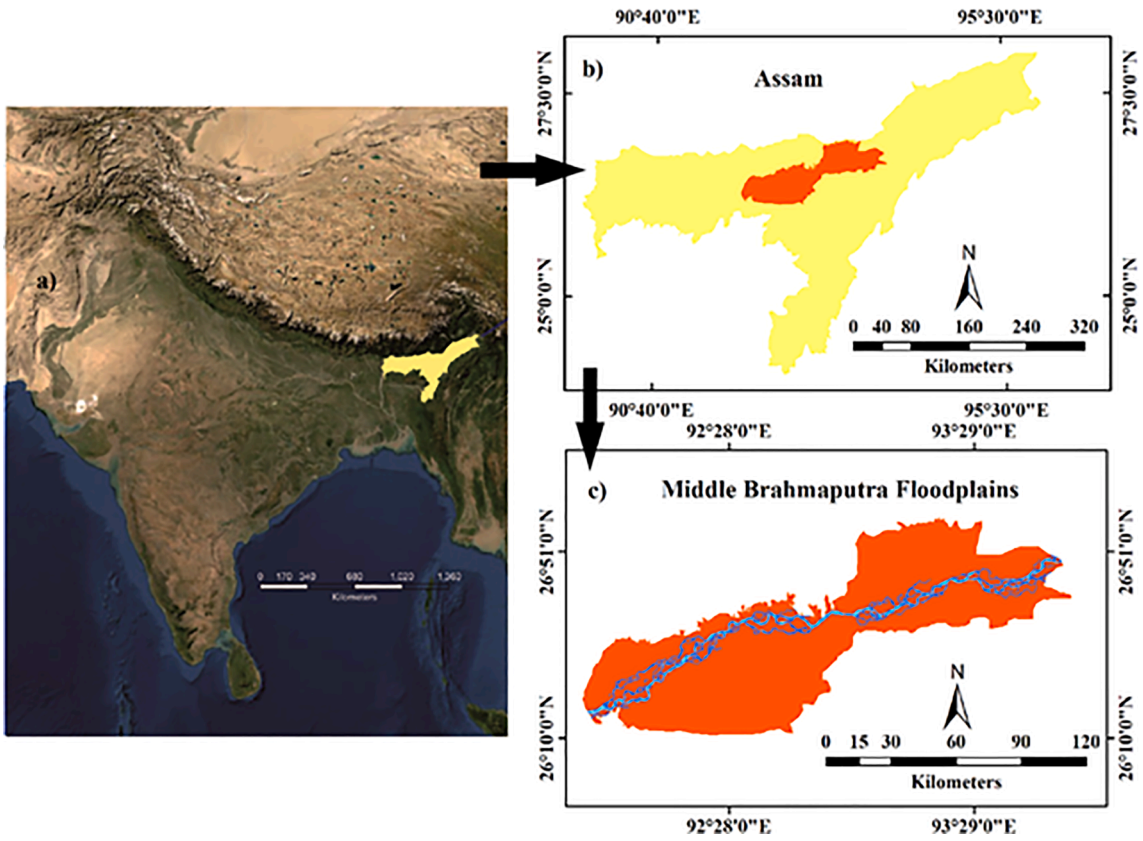

Fig. 1. Location of study area.

the plains and develops an expansive drainage network which is representative of dendritic and trellis drainage patterns. The river exhibits a dichotomic behaviour as it is called the 'lifeline of Assam' as well as the 'sorrow of Assam'. It sustains the ecological, economic and socio-cultural life of Assam but also causes massive destruction by causing floods and bank erosion. Assam has recorded an annual loss of $20 million as a result of riverbank erosion and about 7 % of land has been lost during the last 50 years (ADB, 2009).

The Brahmaputra River stretches 250 km in the floodplains. Its left bank tributaries include Kolong and Kopili whereas Jia Bharali River is its right bank tributary. The floodplains are located in a tectonically volatile region. The area is underlain with hard crystalline rocks dating back to the pre-Cambrian era (Kumar et al., 2020; Rajmohan & Prathapar, 2013). The floodplains experience a humid climate. The mean annual rainfall in the study area is around 2500 mm. The average annual minimum and maximum temperatures are 16 °C and 39 °C respectively.

The study area is spread over six districts namely Nagaon, Morigaon, Golaghat, Darrang, Sonitpur and Biswanath. The world heritage site of Kaziranga National Park along with other reserves namely Laokhowa Wildlife, Pobitora Wildlife and Orang National Park Sanctuaries are also located in the study area. The tree species namely *sal, Lagerstroemia, Ficus and Terminalia* of moist deciduous forest are commonly found in the study area (Environment and Forest, 2023). It is also home to numerous animals, birds, insects and aquatic life like the one-horned rhinoceros, spotted deer, swamp deer, swamp buffaloes, royal Bengal tiger, bush quail, longbilled vulture, etc. Wetlands are also found like Batha Beel in the floodplains. This study area has an estimated population of over 3 million (Census of India, 2011). The Brahmaputra River which carries a large volume of water inundates the floodplains during monsoon season and causes severe bank erosion and channel shifting. However, when the river retreats during the dry months, it displays a unique braided pattern. Various temporary islands and channel bars are found within the braided channels. Some of these riverine islands are permanently inhabited islands.

3. Methodology

The LEV map for the Middle Brahmaputra floodplains was prepared using eleven site-specific parameters namely mean monthly rainfall, normalized difference vegetation index (NDVI), soil type, vegetation type, LULC, slope, geomorphology, distance from river, elevation, biological richness and disturbance index (Fig. 2, Table 1). These parameters were selected on the basis of prior information on the study area and after conducting a comprehensive literature review (Nath & Medhi, 2021; Pareta et al., 2019; Sarkar, 2017; Sarma, 2005). The machine learning algorithms of ANN-MLP and RF were integrated with the technique of bagging to create ensembles (B-MLP and B-RF) which were employed for assessing LEV to riverbank erosion. The models were validated through the receiver operating characteristic (ROC) curve. Furthermore, sensitivity analysis was conducted based on the better-performing model to ascertain the dominant factors of LEV to riverbank erosion. The mapping unit of the study area was a 30 m spatial resolution grid. Fig. 3 shows the detailed methodology followed for the present study.

3.1. Rationale for selection of parameters

Rainfall is considered one of the major factors causing riverbank erosion (Chakraborty & Saha, 2022; Naimah & Roslan, 2015; Yusoff & Abidin, 2023). High rainfall leads to an increase in the water level of rivers which causes erosion along the rivers (Ross et al., 2019). The average annual rainfall of the study area exceeds 2500 mm which makes it essential to consider rainfall as a primary factor causing bank erosion. The mean monthly rainfall map was prepared based on gridded data obtained from the India Meteorological Department (IMD) using the inverse distance weighting (IDW) method. NDVI and LULC were made

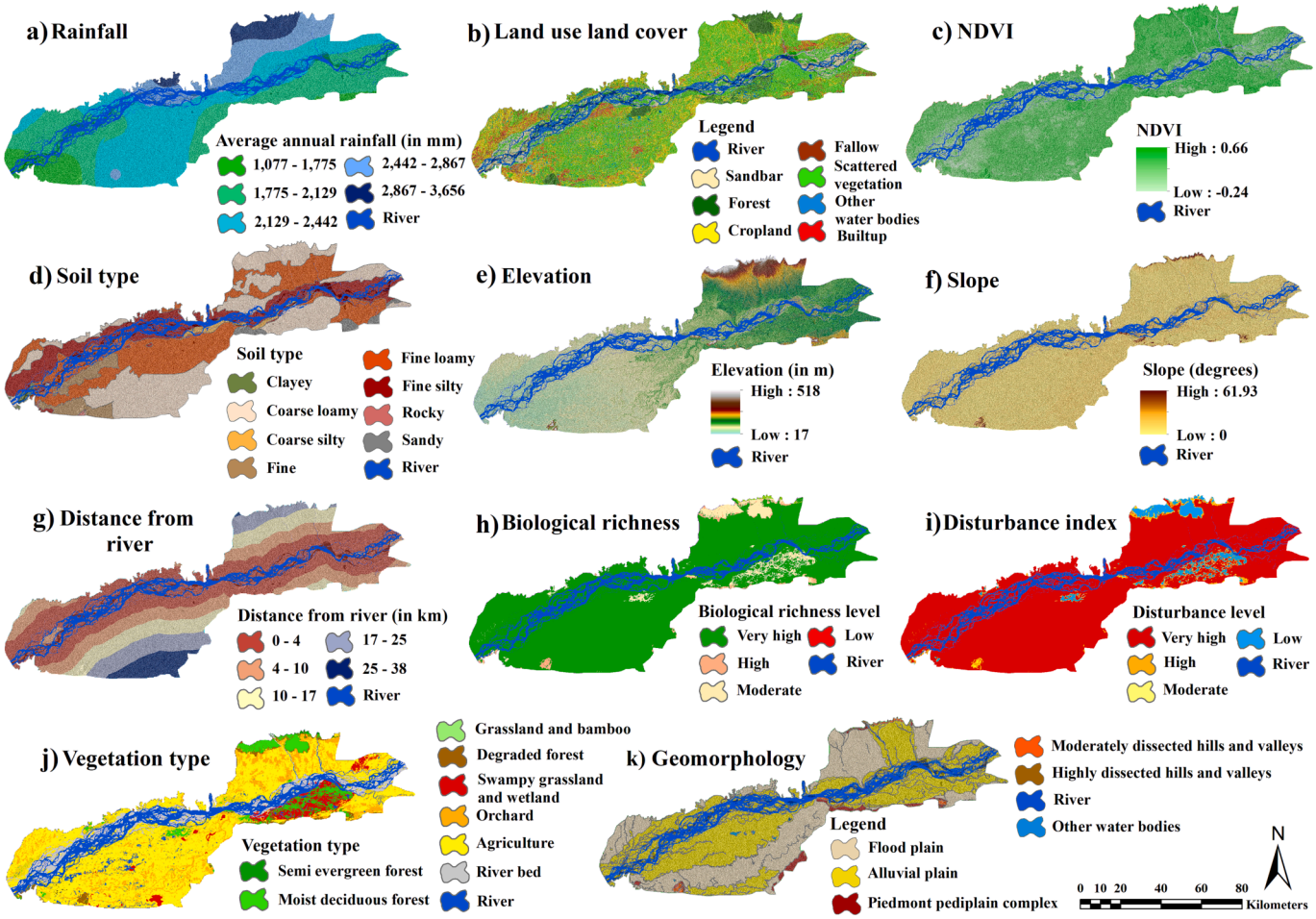

Fig. 2. Parameters for assessing landscape ecological vulnerability: **a)** Rainfall **b)** Land use land cover **c)** NDVI **d)** Soil type **e)** Elevation **f)** Slope **g)** Distance from river **h)** Biological richness **i)** Disturbance index **j)** Vegetation type **k)** Geomorphology.

Table 1
Parameters used for assessment of landscape ecological vulnerability to river-bank erosion.

Parameters	Source of data	Data type	Resolution
Rainfall	Indian Meteorological Department (IMD)	Raster	30 m spatial resolution
Land use land cover	Landsat 8 OLI	Raster	30 m spatial resolution
NDVI	Landsat 8 OLI	Raster	30 m spatial resolution
Soil type	Central Ground Water Board (CGWB)	Vector	1:50,000
Elevation	SRTM DEM (USGS)	Raster	30 m spatial resolution
Slope	SRTM DEM (USGS)	Raster	30 m spatial resolution
Distance from river	Authors' own computation	Raster	30 m spatial resolution
Biological richness	Biological Information System (BIS)	Raster	30 m spatial resolution
Disturbance index	Biological Information System (BIS)	Raster	30 m spatial resolution
Vegetation type	Biological Information System (BIS)	Raster	30 m spatial resolution
Geomorphology	Bhukosh, Geological Survey of India (GSI)	Vector	1:250,000

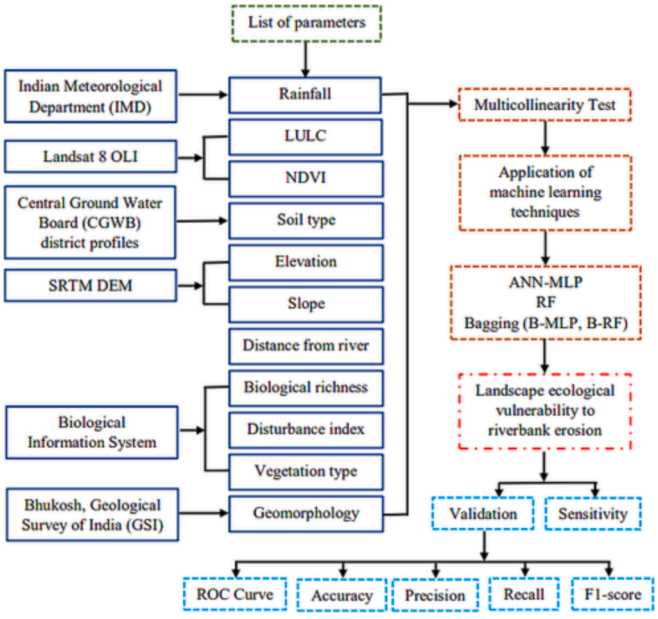

Fig. 3. Methodological flowchart.

on Google Earth Engine using Landsat 8 OLI satellite images. NDVI reflects the health and density of vegetal cover. A healthier vegetation would hold the soil better resulting in increased soil stability. It is calculated as:

$$NDVI = \frac{NIR - Red}{NIR + Red} \quad (1)$$

where *NIR* is near infrared band and *Red* is red band. Changes in LULC impact the hydrological nature of an area and intensify erosion, thereby making it an important parameter for vulnerability assessment (Prashanth et al., 2023). The soil type map was obtained from the Central Ground Water Board district profiles and refurbished according to the need of the study using the ArcGIS software. The type of soil plays an important role in the erodibility of bank materials (Bhowmik, 2018).

Biological richness, Vegetation types and disturbance index maps were prepared based on the data obtained from BIS, Indian Institute of Remote Sensing, India. The types of vegetation were identified in accordance with Champion and Seth's (1968) classification through ground control points (GCPs) and visual interpretation (Roy et al., 2012; Roy et al., 2015). Riverbank erosion is strongly related with vegetation. The changes in shear stress are caused due to presence of vegetation (Gholami & Khaleghi, 2013). Vegetation with stronger and deeper roots tends to hold the soil better and reduces the chances of erosion. Thus, the type of vegetation has the potential to determine the level of erodibility of the different areas. Uniqueness, richness and relevance of species, ecosystem uniqueness, the value of biodiversity, disturbance, and terrain attributes were used to create biological richness spatial layer (Behera et al., 2005, Behera & Roy, 2010). Biological richness helps in demarcating areas with species abundance and the conservation of such areas (BIS, 2020). Disturbance index was determined by combining matrices like porosity, fragmentation, interspersion and juxtaposition. Probabilistic weightage was assigned to the indicators by applying linear combination method to create this spatial layer (Roshani et al., 2022a, Roshani et al., 2022b). It is effective in identifying the disturbance created by human-induced activities on the landscape and ecosystem.

Shuttle radar topography mission digital elevation model (SRTM DEM) was utilized for preparing slope and elevation maps. Slope is a significant factor that needs consideration while assessing vulnerability to riverbank erosion (Macfall et al., 2014). Similarly, elevation also plays an active role in ascertaining the degree of vulnerability to bank erosion. The regions of higher elevation would have a lesser possibility of erosion than the low-lying areas (Saikia & Goswami, 2020).

The geomorphology map was derived from the Geological Survey of India's digital database portal of Bhukosh. The study area is divided into seven geomorphological units namely flood plain, alluvial plain, pediment pediplain, moderately dissected hills and valleys, highly dissected hills and valleys, river and other water bodies. The geomorphological setup of an area would determine its erodibility wherein the newer floodplains formed with loose and unconsolidated silt are likely to get easily eroded. Distance from river was calculated using the Euclidean distance method in ArcGIS. The area closest to the river would have a higher risk of getting eroded compared to the regions located farther away from the river (Singha et al. 2020).

3.2. Riverbank erosion inventories

In order to prepare LEV modelling, a collection of historical riverbank erosion events is needed. Riverbank erosion vulnerability zones were created on the basis of past bank erosion and its conditioning factors. It is essential to generate riverbank erosion inventories to train and evaluate the model. The current study identified the locations of riverbank erosion with the help of data generated from field survey and government report. Global positioning system (GPS) and Google Earth were used to select 260 bank erosion-prone sites. Of the total number of selected sites, 208 sites (80 %) were used to create training datasets whereas the other 52 sites (20 %) were utilized for creating testing datasets. This selection was done on a random basis. Since the present study relied on classification-dependent bank erosion mapping that includes binary data, areas not vulnerable to bank erosion were also marked. The same number of negative points could be used to obtain satisfactory results (Tang et al., 2020). Therefore, 200 sites which are not prone to erosion were also chosen randomly which included 160 training and 40 testing datasets. The ratio of training to testing datasets in both cases was 80:20. 80 % of all bank erosion and non-bank erosion sites were used to determine training datasets. Binary training datasets were created by assigning 0 value to bank erosion points and 1 to non-bank erosion points. Similarly, testing datasets were generated in a binary pattern. Further, data was extracted from riverbank erosion conditioning factors for training the models.

3.3. Multicollinearity test

LEV to riverbank erosion was assessed on the basis of eleven parameters. It is necessary to examine the collinearity of the selected parameters for determining vulnerability since machine learning functions are affected by collinearities wherein the accuracy of the assessment is reduced (Alqadhi et al., 2021). Running a multicollinearity test ensures that the redundant factors are filtered out (Talukdar et al., 2020). Tolerance and variance inflation factor were used in estimating multicollinearity among the chosen parameters which are calculated as.

$$T = 1 - r^2 \quad (2)$$

$$VIF = 1/T \quad (3)$$

where T is tolerance and VIF is variance inflation factor. If the value of VIF is more than 10 and T is less than 0.1, it suggests a multicollinearity issue (Saha et al., 2017; Saha et al., 2021a, Saha et al., 2021b. Collinearity and VIF are directly proportional to each other, that is, higher collinearity would mean a bigger VIF. In the present study, no collinearity was found among the variables. Hence, none of the parameters was excluded from the vulnerability analysis.

3.4. Machine learning methods

In the present study, two machine learning techniques were used namely artificial neural network-multilayer perceptron (ANN-MLP) and random forest (RF). Bagging algorithms for MLP and RF were created by integrating ANN-MLP and RF.

3.4.1. Artificial neural network-multilayer perceptron (ANN-MLP)

ANN is a machine learning approach and was developed on the basis of the working of a human brain (Saha et al., 2021a, Saha et al., 2021b). It is inspired by a complex interconnectedness of neurons joined together by several nodes. MLP is an intrinsic constituent of ANN which has been employed for various hazard modelling (Alqadhi et al., 2022a, Alqadhi et al., 2022b). It is inclusive of three elements, that is, input, hidden and output layers (Masroor et al., 2023; Park & Lek, 2016). The neurons gather inputs, process and transfer the result further onto another network. This leads to a one-directional passage of data from the input layer to the hidden layer to the output layer (Khatun et al., 2021). Non-linear combinations input variables and the training data were utilized in MLP for creating the ecological model.

3.4.2. Random forest (RF)

Random forest (RF) is a non-parametric machine learning method that relies on decision trees. Apart from prediction and time series forecasting, it is used for classification purposes (Polikar, 2012; Qiu et al., 2017; Saha et al., 2021a, Saha et al., 2021b). The current study used RF for evaluating LEV to riverbank erosion. Training data from the original dataset was randomly selected and used to develop the model

for the present study. The execution of various models is supported by the enhancement of the attributes of the model. Decision trees are created by RF wherein every tree is built by using the bootstrap training samples (Breiman, 2001). The parameters and number of decision trees to be chosen and assessed must be predetermined. The expansion of the trees aids in reducing classification errors. Eventually, the final outcome was created by integrating the outcomes of the classification of all decision trees. RF can effectively manage huge datasets and precisely ascertain the importance of parameters (Roshani et al., 2022a, Roshani et al., 2022b). It is also relatively less affected by multicollinearity and can cope with missing and skewed data (Mahato et al., 2021).

3.4.3. Bagging

MLP and RF were integrated with bagging for creating ensembles of bagging-MLP and bagging-RF (B-MLP and B-RF) for modelling LEV to riverbank erosion. Firstly, a bagging algorithm was used for enhancing the training datasets, followed by the use of base classifier for classifying riverbank erosion vulnerability. The final model was created by employing bootstrap sampling from the training data and integrating base classifiers (Breiman 1996). This method generates bootstrap samples by considering the training datasets wherein some samples are emulated and few are replaced (Saha et al., 2022). The bootstrapped sub-datasets (bootstrap samples) were utilized to construct based learners. Further, the majority voting strategy is used to combine the learners. The WEKA software was used to construct the B-MLP and B-RF models. The parameters optimization of the utilized machine learning ensembles is presented in Table 2.

3.5. Accuracy assessment

The ROC-based AUC, accuracy, precision, recall and F1-score using positive and negative sample sets were utilized to assess the performance of the applied models. These popular metrics are used for assessing model accuracy (Liao et al. 2022). The ROC curve is a graphical representation that illustrates the performance of a binary classification model. Positive samples were selected from the predicated model and where LEV actually occurred while negative sample sets were selected from the predicated model and where LEV was not found. Higher ROC values reflect a better-performing model (Liu et al. 2023; Masroor et al., 2023). The area under the curve (AUC) of the ROC curve exhibits the goodness of fit and expresses the accuracy of the models (Mahato et al., 2021). Generally, the AUC value is between 0 and 1. The value of 1 is the marker of a precise analytical test whereas 0 identifies the result as wrong. The values of AUC were grouped into five categories by Rasyid et al. (2016) as excellent (0.9–1.0), good (0.8–0.9), fair (0.7–0.8), poor (0.6–0.7) and fail (0.5–0.6). For computing the ROC curve, sensitivity is plotted on the Y-axis and specificity along the X-axis. Sensitivity indicates false positive and specificity shows false negative. It was derived as:

$$Sensitivity = \frac{TP}{(TP + FN)} \tag{4}$$

$$Specificity = \frac{TN}{(TN + FP)} \tag{5}$$

Accuracy is the ratio of the precisely identified pixels to the total pixels.

Table 2
Parameters optimization of utilized machine learning models.

Models	Description of optimized parameters
B-MLP	Hidden layer-11, Batch size-100, Learning rate-0.3, Seed-5, Momentum-0.2, Training time-1.57 s, Normal to binary filter-TRUE, Validation threshold-20
B-RF	Batch size-100, Number of iteration-100, Max depth-1, Seed-1, Compute attribute importance-TRUE, Calc out of bag-TRUE

Precision refers to the ratio of the accurately identified positive pixels to the total identified positive pixels. Recall is the ratio of accurately classified positive pixels to all pixels in a category. F1-score is derived using the harmonic mean of recall and precision. These metrics deliver a thorough assessment of the model's performance (Kilichev & Kim 2023; Liao et al. 2022). The metrics are calculated as follows:

$$Accuracy = \frac{TP + TN}{TP + TN + FP + FN} \tag{6}$$

$$Precision = \frac{TP}{TP + FP} \tag{7}$$

$$Recall = \frac{TP}{TP + FN} \tag{8}$$

$$F1 - score = \frac{2Precision*Recall}{Precision + Recall} \tag{9}$$

where *TP* represents the true positive, *TN* represents the true negative, *FP* indicates the false positive and *FN* indicates the false negative. The appropriately classified positive and negative pixels into positive and negative categories are represented by the *TP* and the *TN* while the incorrectly classified pixels are shown by the *FP* and the *FN*.

3.6. Sensitivity analysis

Sensitivity analysis was carried out for the model which delivered the best results. To understand the relevance of the factors in spatial and numerical terms, the model was run over and over by cumulatively excluding the factors. For instance, there are a total of eleven parameters (P_1, P_2……P_{11}). For conducting sensitivity analysis, the first parameter, P_1, was excluded and the model was run by considering only the remaining ten parameters. Similarly, two parameters, P_1 and P_2 were excluded in the next step and so on. All the parameters were excluded in consecutive steps until the last model was run with only one parameter, P_{11}. The AUC value is calculated for each of these models and then compared with the AUC value of the model which was generated using all the parameters. Those cases where the removal of a parameter created the maximum difference in the AUC could be regarded as the dominant determining attribute of vulnerability.

4. Results

4.1. Assessment of landscape ecological vulnerability to riverbank erosion

Two machine learning techniques viz., B-MLP and B-RF were used to assess LEV of the study area to riverbank erosion (Fig. 4). A multicollinearity test was conducted to filter out the unnecessary parameters since collinearity among the variables leads to poor performance of the machine learning models. Tolerance and VIF were calculated for each of the 11 parameters (Table 3). LULC had the lowest VIF value (1.38) while disturbance index had the highest VIF value (5.91). It was found that none of the 11 factors were influenced by collinearity and all the 11 parameters could be used to assess LEV to riverbank erosion. Five classes of vulnerability (very high, high, moderate, low and very low vulnerability) were created for each model. Table 4 shows the area (in per cent and km^2) under each vulnerability zone. The vulnerability modelling carried out using B-MLP and B-RF revealed that the maximum area of the floodplains was very highly vulnerable to riverbank erosion. The B-MLP ensemble model measured the largest area under very high vulnerability (28.04 %) followed by very low (23. 54 %), low (17.55 %), high (16.81 %) and moderate (14.07 %). Similar results of level of vulnerability were shown by B-RF, except low and very low categories of vulnerability with minor changes.

The results showed that the southern bank of the river was more vulnerable compared to the northern bank. The level of vulnerability

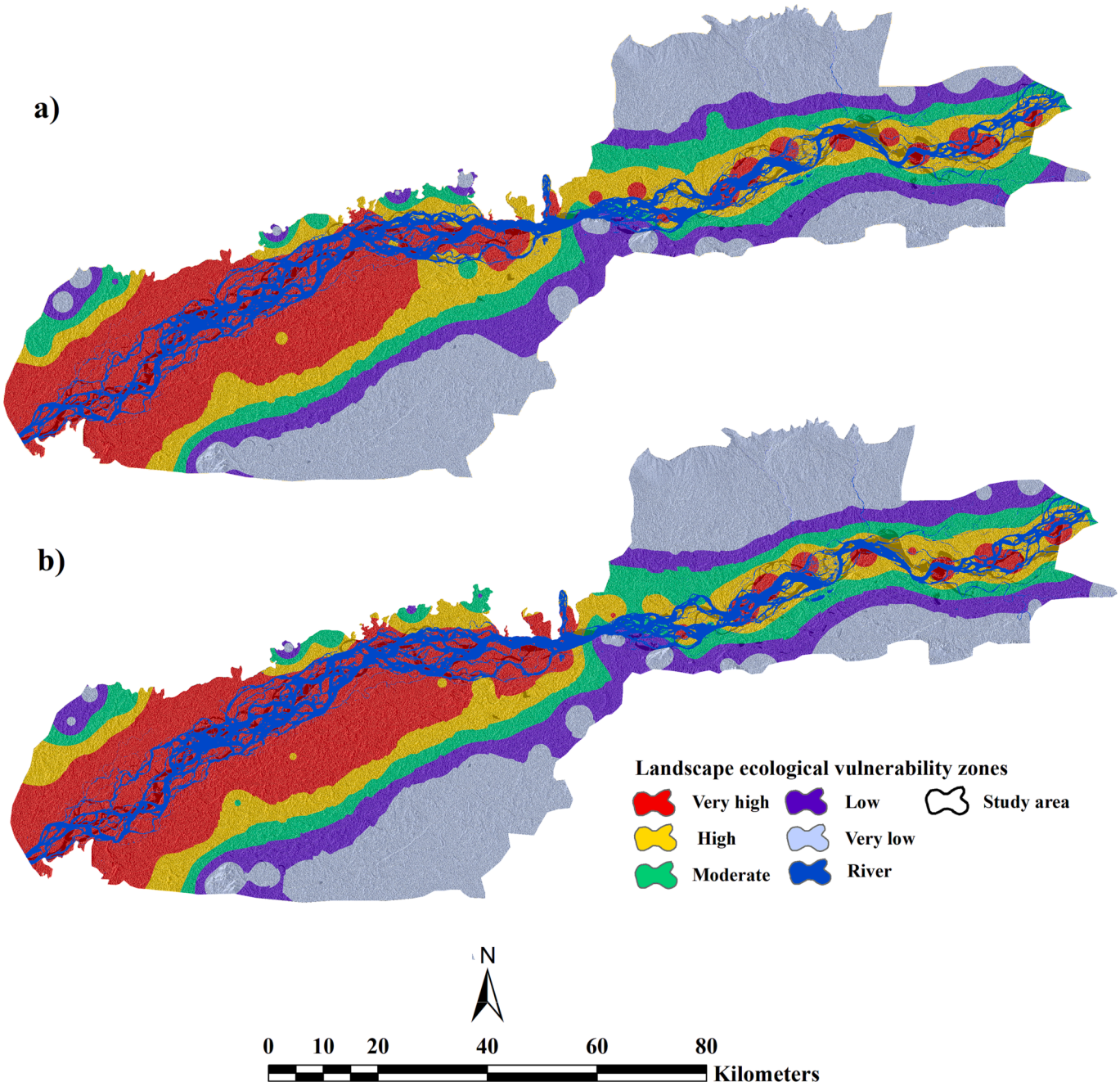

Fig. 4. Landscape ecological vulnerability zones: **a)** B-MLP and **b)** B-RF.

Table 3
Multi-collinearity test of different factors.

Factors	Collinearity statistics	
	Tolerance	VIF
Rainfall	0.45	2.25
NDVI	0.43	2.33
Soil type	0.65	1.54
Vegetation type	0.23	4.37
LULC	0.73	1.38
Slope	0.52	1.93
Geomorphology	0.56	1.78
Distance from river	0.60	1.66
Elevation	0.34	4.24
Biological richness	0.22	4.47
Disturbance index	0.23	4.91

was reduced with an increased distance from the river. The very highly vulnerable areas were located along and within the river channel. The area along the river in the south-western part of the floodplains is very highly vulnerable to bank erosion. Very high vulnerable areas were also located along the north-western part of the study area, however, the expanse of very high vulnerable zone was more along the southern bank. In the eastern part of the floodplains, very highly vulnerable areas were concentrated mostly within the river channel. The highly vulnerable areas were located relatively farther away from the river, next to the very high vulnerable zone. Similarly, the moderately vulnerable regions were located next to the highly vulnerable areas. The majority of the areas in the eastern part of the study area have low vulnerability to riverbank erosion. Moreover, the fringes of the study area represented regions of low vulnerability.

Table 4
Area under different landscape ecological vulnerability zones.

Vulnerability zones	B-MLP			B-RF		
	Pixel count	Area (%)	Area (km^2)	Pixel count	Area (%)	Area (km^2)
Very high	2,381,138	28.04	2045.27	2,171,881	25.58	1865.84
High	1,427,426	16.81	1226.14	1,568,911	18.46	1346.49
Moderate	1,194,728	14.07	1026.28	1,389,719	16.37	1194.05
Low	1,490,271	17.55	1280.12	1,726,023	20.33	1482.89
Very low	1,998,973	23.54	1717.04	1,636,002	19.27	1405.58

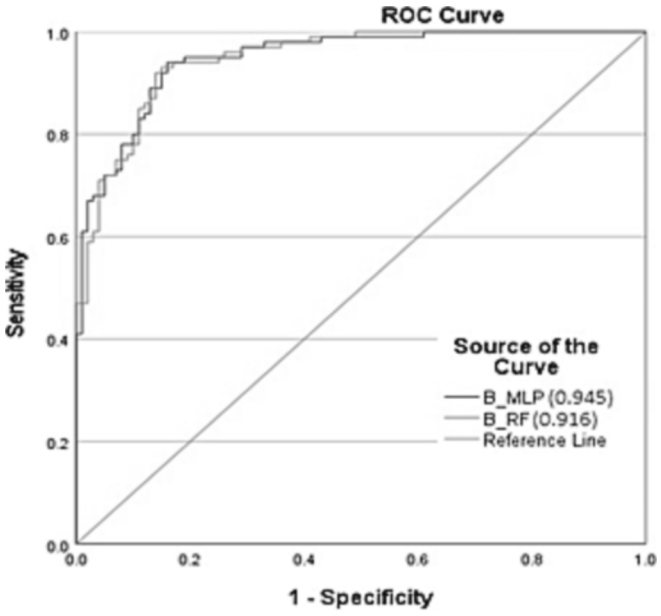

Fig. 5. ROC curve for the landscape ecological vulnerability models.

4.2. Validation of models

The two models were validated using the ROC curve, accuracy, precision, recall and F1-score. Fig. 5 shows the ROC curves for the models. The AUC values of the ROC curve indicate the alignment between the models used and the real scenario (Alqadhi et al., 2022a, Alqadhi et al., 2022b). The higher the calculated values of the metrics, that is, nearer to 1.0, the better the model's performance (Kilichev & Kim 2023; Parvin et al., 2022). The B-MLP had a higher AUC value of 0.945, followed by B-RF (0.916) (Table 5). If the AUC value is estimated to be greater than 0.70, it suggests that the results of the model and ground reality are well aligned (Talukdar et al., 2021). In addition to the AUC values of the ROC curve, B-MLP also performed better based on the values of accuracy (0.864), precision (0.909), recall (0.854) and F1-score (0.881). B-RF also recorded excellent accuracy (0.846), precision (0.884), recall (0.850) and F1-score (0.867) scores. Both the models delivered effective results for analysing LEV to riverbank erosion. However, based on the calculated metrics values, B-MLP was found to be the better-performing model than B-RF.

Table 5
Performance of B-MLP and B-RF models.

Metrics	B-MLP	B-RF
AUC	0.945	0.916
Accuracy	0.864	0.846
Precision	0.909	0.884
Recall	0.854	0.850
F1-score	0.881	0.867

4.3. Sensitivity analysis

The sensitivity analysis helped in identifying the most and least influential factors for LEV to riverbank erosion (Saha et al., 2021a, Saha et al., 2021b). The model validation through the ROC curve revealed that the B-MLP model performed better than the B-RF model. Hence, sensitivity analysis was conducted for B-MLP. A total of 11 parameters were chosen for the study, therefore, the model was run 10 times wherein, one parameter was excluded at each consecutive step. Fig. 6 shows the changes in the spatial distribution of riverbank erosion vulnerability zones after the exclusion of parameters in a cumulative way. The calculation of AUC values indicated the extent to which the model was impacted due to the exclusion of the LEV factors (Table 6). The analysis showed that rainfall, NDVI, soil type, vegetation type and LULC were important factors which determined LEV to riverbank erosion. The removal of these factors significantly lowered the level of accuracy of the model (AUC: 0.756 to 0.0.853). On the other hand, factors like disturbance index and biological richness had a lesser impact on LEV.

5. Discussion

The Middle Brahmaputra floodplains are highly vulnerable to riverbank erosion caused by rainfall, vegetation types, soil types and LULC in the study area. The floodplains receive over 2500 mm of rainfall on average annually. Higher rainfall leads to more volume of water in the river which increases the erosive capacity of the river. Precipitation is the main source of water for the Brahmaputra River. The river inundates its banks due to the occurrence of incessant rains and causes severe bank erosion (Singh, 2008). The Brahmaputra transports huge quantities of sediments and deposits the silt along its banks. The soils on the riverbanks are composed of unconsolidated materials like silt and fine sand which are easily erodible (Kataki et al., 2017; Nath & Medhi, 2021; Sarma, 2005). It was noticed that the vulnerability decreased as the distance from the river increased. Riverbank erosion is a function of the wearing away of bank materials by the action of running water. It is also observed that the areas along the river channel experienced more vulnerability as compared with the fringe areas. The western part of the floodplains was found to be more vulnerable to bank erosion than the eastern part. The very high vulnerable zone was found in a stretch extending for 10–12 km from the river in the south-west of the floodplains.

The south-western and north-western parts of the study area along the river were very highly vulnerable to erosion. These areas are characterized by scattered vegetation and agricultural fields. Low NDVI indicated poor health and less density of vegetation in these areas. A higher NDVI shows healthier vegetation and vice-versa. Values ranging between 0.2 and 0.5 indicate grasslands and shrubs whereas higher values between 0.6 and 0.8 show the presence of tropical and temperate forests (NASA Earth Observatory, 2000; USGS, 2018). The range of NDVI values in the present study was −0.24 to 0.66. The regions which recorded NDVI values less than 0.3 were found to be more vulnerable since these regions primarily included shrubs, grasslands and barren areas. On the other hand, the forested areas with NDVI values of 0.6 or more were less vulnerable to bank erosion. The roots of trees and healthy

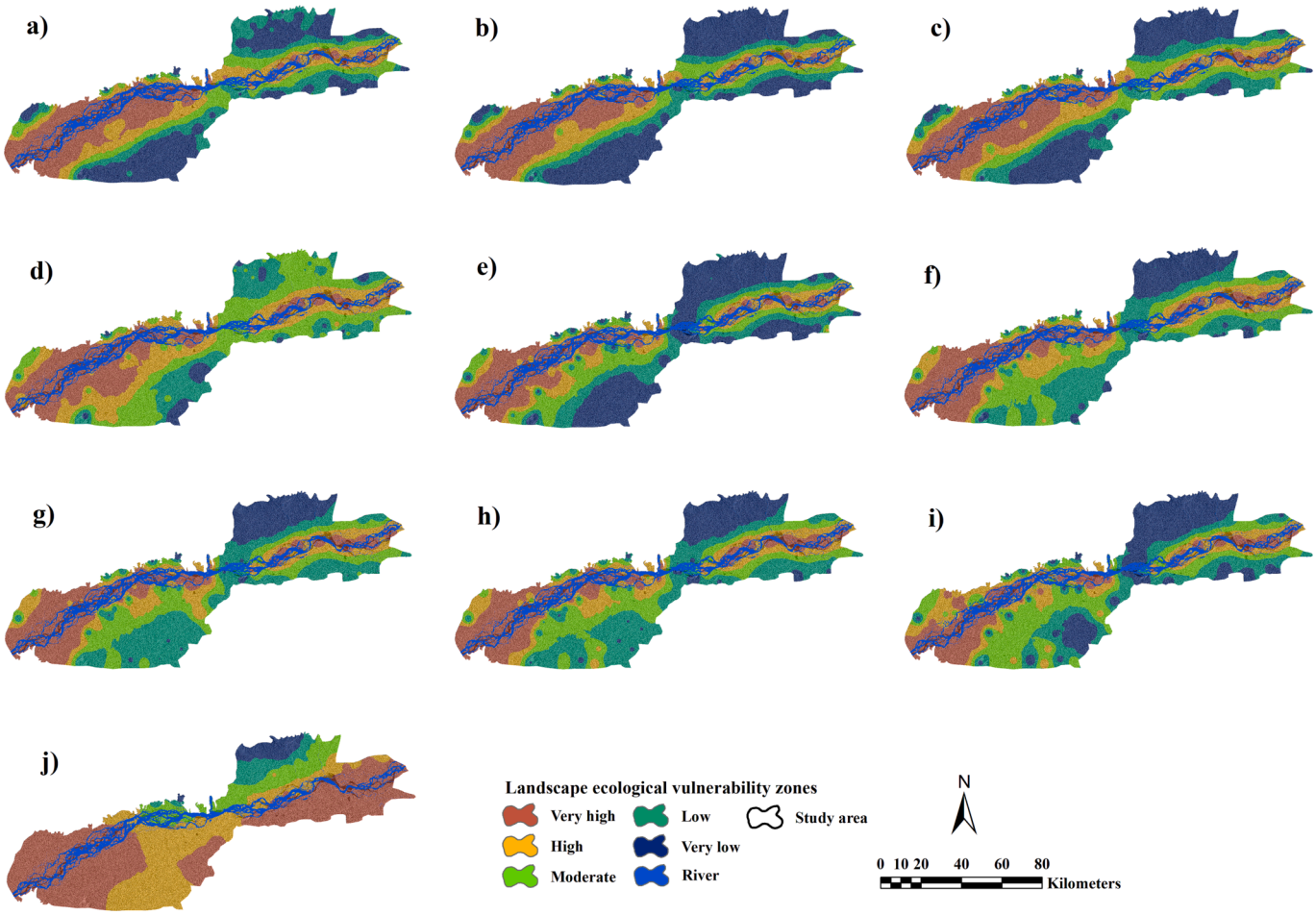

Fig. 6. B-MLP based landscape ecological vulnerability zones post exclusion of parameters of: **a)** DI **b)** DI and BR **c)** DI, BR and Elevation **d)** DR, BR, Elevation and Distance from river **e)** DI, BR, Elevation, Distance from river and Geomorphology **f)** DI, BR, Elevation, Distance from river, Geomorphology and Slope **g)** DI, BR, Elevation, Distance from river, Geomorphology, Slope and LULC **h)** DI, BR, Elevation, Distance from river, Geomorphology, Slope, LULC and VT **i)** DI, BR, Elevation, Distance from river, Geomorphology, Slope, LULC, VT and ST **j)** DI, BR, Elevation, Distance from river r, Geomorphology, Slope, LULC, VT, ST and NDVI.

Table 6
AUC of ROC for sensitivity analysis.

Factor(s) exclusion	AUC	AUC departure due to exclusion
DI	0.938	0.007
DI + BR	0.932	0.006
DI + BR + Elevation	0.913	0.019
DI + BR + Elevation + Distance from river	0.881	0.032
DI + BR + Elevation + Distance from river + Geomorphology	0.879	0.002
DI + BR + Elevation + Distance from river + Geomorphology + Slope	0.853	0.026
DI + BR + Elevation + Distance from river + Geomorphology + Slope + LULC	0.803	0.05
DI + BR + Elevation + Distance from river + Geomorphology + Slope + LULC + VT	0.782	0.021
DI + BR + Elevation + Distance from river + Geomorphology + Slope + LULC + VT + ST	0.771	0.011
DI + BR + Elevation + Distance from river + Geomorphology + Slope + LULC + VT + ST + NDVI	0.756	0.015

DI = Disturbance index, ***BR*** = Biological richness, ***LULC*** = Land use land cover, ***VT*** = vegetation type, ***ST*** = Soil type.

vegetation would hold on to the soil more strongly, thereby making the area less susceptible to erosion (Holanda et al., 2005). The LULC map showed the dominance of croplands and scattered vegetation in the study area. The soils are less likely to be eroded due to the absence of strong and deep roots of the riparian vegetation. On the other hand, the south-eastern parts of the floodplains have higher vegetation moist deciduous and swampy forests. The LULC map also showed that south-eastern bank consists of dense forest areas. The north-eastern parts were dotted with orchards and deciduous trees. These parts are characterized by trees namely *Dalbergia sissoo, Bombax ceiba, Gmelina arborea*, *Tetrameles nodiflora* and *Samanea saman,* these trees have deeper routes which helped the soil to become compact and thus made these areas relatively less vulnerable to erosion. This finding is in tune with Guha (2021). However, the eastern part of the floodplains is less vulnerable to bank erosion compared to the western part since the former has a relatively higher elevation. The western part of the study area is also prone to more disturbance as revealed by the disturbance index.

The study noted that the southern bank was more vulnerable to bank erosion than the northern bank. Saikia et al. (2019) and Sarkar et al. (2012) inferred from their studies that riverbank erosion was more pronounced along the left bank of the river and the Brahmaputra's bank line was shifting southwards. The southern bank is composed of newer alluvium which could be conveniently eroded away and eroded quickly. The northern bank has a higher elevation than the southern bank, thereby making the left bank more vulnerable to erosion. Some areas, though closer to the river, have low vulnerability due to the presence of dissected hills containing gneiss and quartzite (Kotoky et al., 2009; Sarma & Phukan, 2006). A risk assessment study carried out by Sharma et al. (2010) also found that the southern bank was more prone to

riverbank erosion. Rainfall, vegetation, soil, elevation and geomorphology were the major factors that contributed to LEV. The eleven parameters used for constructing the B-MLP and B-RF models were processed in the WEKA software. This software uses distinct algorithms to learn patterns from the data. These algorithms work differently for different types of data. The hyperparameters and their characteristics were different, thus, the results obtained through both models were different. However, the results were close for both models.

More focus could be laid on those aspects which intensify riverbank vulnerability the most and mitigation strategies could be framed accordingly. The 'Molai Kathoni' model which relies on creating planted trees along riverbanks is considered an effective step towards protecting lands from getting eroded (Guha 2021). The cultivation of indigenous plant varieties like bamboo makes the soil more resilient to bank erosion. Construction of embankments and permeable structures like cribs and porcupines also help reduce rates of erosion. Other techniques like the use of geobags, geotextile tube embankment construction and bioengineering would prove beneficial in controlling bank erosion, thereby reducing vulnerability. Fig. 7 shows the riverbank erosion scenario in the study area and the measures taken to restrict riverbank erosion.

Limitations of the study

The present study has laid out a comprehensive framework for the assessment of LEV to riverbank erosion, however, there exist some drawbacks like employing satellite images with moderate resolution, utilizing a semi-quantitative approach due to shortage of data and using

Fig. 7. A) to C) Erosion along the banks of the Brahmaputra **D)** Porcupines and geobags to protect banks from erosion **E)** and **F)** Embankments to secure banks from further erosion.

lesser bank erosion sites for modelling. Algorithm hyperparameters also influenced the performance of the model. Optimization of parameters in B-MLP and B-RF models was tuned until optimal results were obtained. Thus, this assessment could be further improved if the above limitations are overcome. Nevertheless, the methods applied in this study proved efficient and could be used by other spatial units for effective assessment of LEV to riverbank erosion by adopting indicators relevant to the respective study areas.

6. Conclusion

The study examined LEV to riverbank erosion in the Middle Brahmaputra floodplains of Assam, India. A total of eleven site-specific indicators were chosen for the assessment based on a comprehensive review of literature and prior knowledge of the study area. The parameters included rainfall, NDVI, soil type, vegetation type, LULC, slope, geomorphology, distance from river, elevation, biological richness and disturbance index. Two ensembles of machine learning namely B-MLP and B-RF were used for generating LEV to riverbank erosion maps. The models were validated using the ROC curve. The ROC curve-based AUC, accuracy, precision, recall and F1-score values suggested that B-MLP was the better-performing model (AUC = 0.945, accuracy = 0.864, precision = 0.909, recall = 0.854, and F1-score = 0.881). The results revealed that the largest area of the floodplains based on B-MLP was found under the very high vulnerability zone (28 %) followed by very low (23 %), low (17 %), high (17 %) and moderate (14 %) vulnerability zones. The western part of the study area was more vulnerable to riverbank erosion than the eastern region. Moreover, the southern bank of the river was relatively more prone to bank erosion compared to the northern bank. The sensitivity analysis showed that factors namely rainfall, soil type, vegetation type and LULC influenced bank erosion vulnerability in this study area. Plantation of trees, embankment construction and the use of bioengineering and geotextile technologies could be harnessed to protect the banks from further erosion. This study may help local stakeholders and conservationists in devising adequate measures for managing riverbank erosion.

CRediT authorship contribution statement

Nirsobha Bhuyan: Conceptualization, Data curation, Software, Methodology, Validation. **Haroon Sajjad:** Conceptualization, Supervision. **Tamal Kanti Saha:** Conceptualization, Software, Methodology, Validation. **Roshani:** . **Yatendra Sharma:** Data curation. **Md Masroor:** Data curation. **Md Hibjur Rahaman:** Formal analysis, Visualization, Investigation. **Raihan Ahmed:** Formal analysis, Visualization, Investigation.

Declaration of Competing Interest

The authors declare that they have no known competing financial interests or personal relationships that could have appeared to influence the work reported in this paper.

Data availability

Data will be made available on request.

Acknowledgements

The authors express deep gratitude to the United States Geological Survey (USGS) for providing satellite images. The authors are grateful to the anonymous reviewers for their insightful comments and meaningful suggestions to improve the overall quality of the work.

References

ADB, 2009. Environmental Assessment Report. Summary Environmental Impact Assessment. Project Number: 38412, India: Assam Integrated Flood and Riverbank Erosion Risk Management Investment Program.

Ado, M., Amitab, K., Maji, A.K., Jasińska, E., Gono, R., Leonowicz, Z., Jasiński, M., 2022. Landslide susceptibility mapping using machine learning: A literature survey. Remote Sens. 14, 3029. https://doi.org/10.3390/rs14133029.

Ahmed, I., Das, N., Debnath, J., Bhowmik, M., 2018. Erosion induced channel migration and its impact on dwellers in the lower Gumti River, Tripura. India. Spat. Inf. Res. 26, 537–549. https://doi.org/10.1007/s41324-018-0196-9.

Ahmed, A.A., Fawzi, A., 2011. Meandering and bank erosion of the River Nile and its environmental impact on the area between Sohag and El-Minia. Egypt. Arab. J. Geosci. 4, 1–11. https://doi.org/10.1007/s12517-009-0048-y.

Ai, J., Yu, K., Zeng, Z., Yang, L., Liu, Y., Liu, J., 2022. Assessing the dynamic landscape ecological risk and its driving forces in an island city based on optimal spatial scales: Haitan Island. China. Ecol. Indic. 137, 108771 https://doi.org/10.1016/j.ecolind.2022.108771.

Al-Areeq, A., Abba, S., Yassin, M., Benaafi, M., Ghaleb, M., Aljundi, I., 2022. Computational machine learning approach for flood susceptibility assessment integrated with remote sensing and GIS techniques from Jeddah, Saudi Arabia. Remote Sens. 14, 5515. https://doi.org/10.3390/rs14215515.

Alqadhi, S., Mallick, J., Talukdar, S., Bindajam, A.A., Saha, T.K., Ahmed, M., Khan, R.A., 2022a. Combining logistic regression-based hybrid optimized machine learning algorithms with sensitivity analysis to achieve robust landslide susceptibility mapping. Geocarto International 37, 9518–9543. https://doi.org/10.1080/10106049.2021.2022009.

Alqadhi, S., Mallick, J., Talukdar, S., Bindajam, A.A., Van Hong, N., Saha, T.K., 2022b. Selecting optimal conditioning parameters for landslide susceptibility: an experimental research on Aqabat Al-Sulbat, Saudi Arabia. Environmental Science and Pollution Research 29, 3743–3762. https://doi.org/10.1007/s11356-021-15886-z.

Arefin, R., Meshram, S.G., Seker, D.Z., 2021. River channel migration and land-use/land-cover change for Padma River at Bangladesh: a RS- and GIS-based approach. International journal of Environmental Science and Technology 18, 3109–3126. https://doi.org/10.1007/s13762-020-03063-7.

Azarafza, M., Azarafza, M., Akgün, H., Atkinson, P.M., Derakhshani, R., 2021. Deep learning-based landslide susceptibility mapping. Scientific Reports 11, 24112. https://doi.org/10.1038/s41598-021-03585-1.

Behera, M.D., Kushwaha, S.P.S., Roy, P.S., 2005. Rapid assessment of biological richness in a part of Eastern Himalaya: an integrated three-tier approach. Forest Ecology and Management 207, 363–384. https://doi.org/10.1016/j.foreco.2004.10.070.

Behera, M.D., Roy, P.S., 2010. Assessment and validation of biological richness at Landscape Level in part of the Himalayas and Indo-Burma Hotspots using geospatial modeling approach. Journal of the Indian Society of Remote Sensing 38, 415–429. https://doi.org/10.1007/s12524-010-0044-4.

Bhowmik, M., Das, C., Ahmed, I., Debnath, J., 2018. Bank Material Characteristics and its Impact on River Bank Erosion, West Tripura District, Tripura, North-East India. Curr. Sci. 115, 1571–1576. https://doi.org/10.18520/cs/v115/i8/1571-1576.

Bhuiyan, M.A.H., Islam, S.-M.-D.-U., Azam, G., 2017. Exploring impacts and livelihood vulnerability of riverbank erosion hazard among rural household along the river Padma of Bangladesh. Environ. Syst. Res. 6, 25. https://doi.org/10.1186/s40068-017-0102-9.

Bhunia, G.S., Shit, P.K., Pal, D.K., 2016. Channel dynamics associated with land use/cover change in Ganges River, India, 1989–2010. Spatial Information Research 24, 437–449. https://doi.org/10.1007/s41324-016-0045-7.

BIS, 2020. National Biodiversity Characterization at Landscape Level Department of Biotechnology and Department of Space, Ministry of Science and Technology. https://bis.iirs.gov. in/methodology and approach. (Last accessed: 14/04/2023).

Biswas, R., Anwaruzzaman, A.K.M., 2019. Measuring hazard vulnerability by bank erosion of the Ganga river in Malda district using PAR Model. J. Geogr. Environ. Earth Sci. Int. 1–15 https://doi.org/10.9734/jgeesi/2019/v22i130136.

Breiman, L., 1996. Bagging predictors. Machine Learning 24, 123–140. https://doi.org/10.1007/BF00058655.

Breiman, L., 2001. Random forests. Machine Learning 45, 5–32. https://doi.org/10.1023/A:1010933404324.

Burel, F., Lavigne, C., Marshall, E.J.P., Moonen, A.C., Ouin, A., Poggio, S.L., 2013. Landscape ecology and biodiversity in agricultural landscapes. Agriculture, Ecosystems and Environment 166, 1–2. https://doi.org/10.1016/j.agee.2013.01.001.

Census of India, 2011. Office of the Registrar General & Census Commissioner, India. URL https://censusindia.gov.in/census.website/data/population-finder. (Last accessed 06/02/23).

Chakraborty, K., Saha, S., 2022. Assessment of bank erosion and its impact on land use and land cover dynamics of Mahananda River basin (Upper) in the Sub-Himalayan North Bengal, India. SN Appl. Sci. 4, 20. https://doi.org/10.1007/s42452-021-04904-x.

Champion, H.G., Seth, S.K., 1968. Revised Forest Types of India. Gov. India Publ, New Delhi.

Chen, X., Li, Y., Yunhao, Z., 2021. Analytic Hierarchy Process (AHP) to analyze the tropical cyclone risk index of 15 coastal cities in China. In: 2021 International Conference on E-Commerce and E-Management (ICECEM). IEEE, pp. 141–146. https://doi.org/10.1109/ICECEM54757.2021.00036.

Clark, W., 2010. Principles of Landscape Ecology. Nat. Educ. Knowl. 3, 34.

Das, K., Bandyopadhyay, S., De, S.K., 2021. Assessing the Impact of Riverbank Erosion on Land Use/Land Cover along the Lower Reach of Balasan River. West Bengal. J, Indian Geomorphol, p. 9.
Das, T.K., Haldar, S.K., Das Gupta, I., Sen, S., 2014. River Bank Erosion Induced Human Displacement and Its Consequences. Living Rev. Landsc. Res. 8, 1–35. https://doi.org/10.12942/lrlr-2014-3.
Debnath, J., Das (Pan), N., Ahmed, I., Bhowmik, M., 2017. Channel migration and its impact on land use/land cover using RS and GIS: A study on Khowai River of Tripura, North-East India. Egypt. J. Remote Sens. Sp. Sci. 20, 197–210. https://doi.org/10.1016/j.ejrs.2017.01.009.
Deroliya, P., Ghosh, M., Mohanty, M.P., Ghosh, S., Rao, K.H.V.D., Karmakar, S., 2022. A novel flood risk mapping approach with machine learning considering geomorphic and socio-economic vulnerability dimensions. The Science of the Total Environment 851, 158002. https://doi.org/10.1016/j.scitotenv.2022.158002.
Dey, S., Mandal, S., 2019. Assessing channel migration dynamics and vulnerability (1977–2018) of the Torsa River in the Duars and Tal region of eastern Himalayan foothills, West Bengal, India. Spat. Inf. Res. 27, 75–86. https://doi.org/10.1007/s41324-018-0213-z.
Dragicevic, S., Tosic, R., Stepić, M., Nenad, Ž., Novković, I., 2013. Consequences of the river bank erosion in the southern part of the Pannonian Basin: Case study – Serbia and the Republic of Srpska. Forum Geogr. 12, 5–15. https://doi.org/10.5775/fg.2067-4635.2013.008.i.
Dragicevic, S., Stojanović, Ž., Manic, E., Roksandic, M., Stepić, M., Nenad, Ž., Zlatic, M., Kostadinov, S., 2017. Economic Consequences of Bank Erosion in the Lower Part of the Kolubara River Basin. Serbia. Environ. Eng. Manag. J. 16, 381–390.
Dutta, K., Chakraborty, S., 2013. Human aspects of river bank erosion: a case study of Khairkata village, Diana River basin, Jalpaiguri, West Bengal. Geo-Analyst 2013.
Environment and Forest, Biodiversity of Assam. Gov. Assam. URL https://environmentandforest.assam.gov.in/portlets/biodiversity-of-assam-0. (Last accessed: 01/04/2023).
Freihardt, J., Frey, O., 2023. Assessing riverbank erosion in Bangladesh using time series of Sentinel-1 radar imagery in the Google Earth Engine. Natural Hazards and Earth System Sciences 23, 751–770. https://doi.org/10.5194/nhess-23-751-2023.
Gao, H., Song, W., 2022. Assessing the landscape ecological risks of land-use change. International Journal of Environmental Research and Public Health 19, 13945. https://doi.org/10.3390/ijerph192113945.
Gholami, V., Khaleghi, M.R., 2013. The impact of vegetation on the bank erosion (Case study: The Haraz River). Soil Water Res. 8, 158–164. https://doi.org/10.17221/13/2012-SWR.
Ghosh, D., Sahu, A.S., 2018. Problem of river bank failure and the condition of the erosion victims: A case study in Dhulian, West Bengal. India. Regional Science Inquiry 10 (2), 205–214.
Ghosh, D., Sahu, A.S., 2019. Bank line migration and its impact on land use and land cover change: A case study in Jangipur subdivision of Murshidabad District, West Bengal. Journal of the Indian Society of Remote Sensing 47, 1969–1988. https://doi.org/10.1007/s12524-019-01043-0.
Guha, N., n.d. Planted forests can tackle flood and erosion impacts along the Brahmaputra. Mongabay. URL https://india.mongabay.com/2021/11/planted-forests-can-tackle-flood-and-erosion-impacts-along-the-brahmaputra/ (last accessed 17/04/23).
Guite, L.T., Bora, A., 2016. Impact of river bank erosion on land cover in lower Subansiri river flood plain. International Journal of Scientific and Research Publications 6, 480–2250.
Hammami, S., Zouhri, L., Souissi, D., Souei, A., Zghibi, A., Marzougui, A., Dlala, M., 2019. Application of the GIS based multi-criteria decision analysis and analytical hierarchy process (AHP) in the flood susceptibility mapping (Tunisia). Arabian Journal of Geosciences 12, 653. https://doi.org/10.1007/s12517-019-4754-9.
Hazarika, N., Das, A.K., Borah, S.B., 2015. Assessing land-use changes driven by river dynamics in chronically flood affected Upper Brahmaputra plains, India, using RS-GIS techniques. Egypt. J. Remote Sens. Sp. Sci. 18, 107–118. https://doi.org/10.1016/j.ejrs.2015.02.001.
Holanda, F.S.R., Santos, L.G. da C., Santos, C.M. dos, Casado, A.P.B., Pedrotti, A., Ribeiro, G.T., 2005. Riparian vegetation affected by bank erosion in the Lower São Francisco River. Northeastern Brazil. Rev. Árvore 29, 327–336. https://doi.org/10.1590/S0100-67622005000200016.
Hussain, M.A., Chen, Z., Zheng, Y., Shoaib, M., Shah, S.U., Ali, N., Afzal, Z., 2022. Landslide susceptibility mapping using machine learning algorithm validated by persistent scatterer In-SAR technique. Sensors 22, 3119. https://doi.org/10.3390/s22093119.
Kataki, S., Sarma, S., Goswami, U., 2017. Groundwater prospect evaluation in the interfluves of the rivers Brahmaputra and Kolong, Assam using remote sensing and GIS techniques. Int. J. Adv. Remote Sens. GIS 6, 2449–2457. https://doi.org/10.23953/cloud.ijarsg.323.
Khatun, R., Talukdar, S., Pal, S., Saha, T.K., Mahato, S., Debanshi, S., Mandal, I., 2021. Integrating remote sensing with swarm intelligence and artificial intelligence for modelling wetland habitat vulnerability in pursuance of damming. Ecol. Inform. 64, 101349 https://doi.org/10.1016/j.ecoinf.2021.101349.
Kilichev, D., Kim, W., 2023. Hyperparameter optimization for 1D-CNN-based network intrusion detection using GA and PSO. Mathematics 11, 3724. https://doi.org/10.3390/math11173724.
Kotoky, P., Bezbaruah, D., Borah, G.C., Sarma, J., 2009. Do node points play a role in flood proliferation? Current Science 96, 1457–1460.
Kremsa, V.Š., 2021. Sustainable management of agricultural resources (agricultural crops and animals). In: Sustainable resource management. Elsevier, pp. 99–145. https://doi.org/10.1016/B978-0-12-824342-8.00010-9.
Kumar, K.S.A., Thayalan, S., Reddy, R.S., Lalitha, M., Kalaiselvi, B., Parvathy, S., Sujatha, K., Hegde, R., Singh, S.K., Mishra, B.B., 2020. Geology and Geomorphology. Springer International Publishing, pp. 57–79.
Liao, M., Wen, H., Yang, L., 2022. Identifying the essential conditioning factors of landslide susceptibility models under different grid resolutions using hybrid machine learning: A case of Wushan and Wuxi counties, China. Catena 217. https://doi.org/10.1016/j.catena.2022.106428.
Liu, R., Ding, Y., Sun, D., Wen, H., Gu, Q., Shi, S., Liao, M., 2023. Insights into spatial differential characteristics of landslide susceptibility from sub-region to whole-region cased by northeast Chongqing, China. Geomat. Nat. Hazards Risk. 14 https://doi.org/10.1080/19475705.2023.2190858.
Liu, J., Wang, M., Yang, L., 2020. Assessing landscape ecological risk induced by land-use/cover change in a county in China: A GIS- and landscape-metric-based approach. Sustainability 12, 9037. https://doi.org/10.3390/su12219037.
Macfall, J., Robinette, P., Welch, D., 2014. Factors influencing bank geomorphology and erosion of the Haw river, a high order river in North Carolina, since European settlement. PLoS One 9, e110170. https://doi.org/10.1371/journal.pone.0110170.
Mahato, S., Pal, S., Talukdar, S., Saha, T.K., Mandal, P., 2021. Field based index of flood vulnerability (IFV): A new validation technique for flood susceptible models. Geoscience Frontiers 12, 101175. https://doi.org/10.1016/j.gsf.2021.101175.
Mallick, J., Singh, R.K., AlAwadh, M.A., Islam, S., Khan, R.A., Qureshi, M.N., 2018. GIS-based landslide susceptibility evaluation using fuzzy-AHP multi-criteria decision-making techniques in the Abha Watershed, Saudi Arabia. Environment and Earth Science 77, 276. https://doi.org/10.1007/s12665-018-7451-1.
Masroor, M., Sajjad, H., Kumar, P., Saha, T.K., Rahaman, M.H., Choudhari, P., Kulimushi, L.C., Pal, S., Saito, O., 2023. Novel ensemble machine learning modeling approach for groundwater potential mapping in Parbhani district of Maharashtra, India. Water 15, 419. https://doi.org/10.3390/w15030419.
Mondal, M., Haldar, S., Biswas, A., Mandal, S., Bhattacharya, S., Paul, S., 2021. Modeling cyclone-induced multi-hazard risk assessment using analytical hierarchical processing and GIS for coastal West Bengal, India. Regional Studies in Marine Science 44, 101779. https://doi.org/10.1016/j.rsma.2021.101779.
Naimah, Y., Roslan, Z.A., 2015. Forecasting river bank erosion with regards to rainfall erosivity and soil erodibility, in: Roslan, Z.A. (Ed.), pp. 67–77. https://doi.org/10.2495/DMAN150071.
Nath, M.J., Medhi, H., 2021. River Bank Line Shift Caused by Brahmaputra in Morigaon District, Assam. Int J Lakes Rivers.
Pareta, K., Jakobsen, P., Joshi, M., 2019. Morphological Characteristics and Vulnerability Assessment of Alaknanda, Bhagirathi, Mandakini and Kali Rivers, Uttarakhand (India). Am. J. Geophys. Geochem. Geosyst. 5, 49–68.
Park, Y.-S., Lek, S., 2016. Artificial Neural Networks. pp. 123–140. https://doi.org/10.1016/B978-0-444-63623-2.00007-4.
Parvin, F., Ali, S.A., Calka, B., Bielecka, E., Linh, N.T.T., Pham, Q.B., 2022. Urban flood vulnerability assessment in a densely urbanized city using multi-factor analysis and machine learning algorithms. Theoretical and Applied Climatology 149, 639–659. https://doi.org/10.1007/s00704-022-04068-7.
Pathan, S.A., Ashwini, K., Sil, B.S., 2021. Spatio-temporal variation in land use/land cover pattern and channel migration in Majuli River Island, India. Environmental Monitoring and Assessment 193, 811. https://doi.org/10.1007/s10661-021-09614-w.
Paul, A., Bhattacharji, M., 2022. Prediction of landuse/landcover using CA-ANN approach and its association with river-bank erosion on a stretch of Bhagirathi River of Lower Ganga Plain. GeoJournal 88, 3323–3346. https://doi.org/10.1007/s10708-022-10814-1.
Pearson, D., 2020. Key roles for landscape ecology in transformative agriculture using Aotearoa—New Zealand as a case example. Land 9, 146. https://doi.org/10.3390/land9050146.
Pearson, S.M., 2013. Encyclopedia of Biodiversity || Landscape Ecology and Population Dynamics. 488–502. https://doi.org/10.1016/B978-0-12-384719-5.00417-2.
Polikar, R., 2012. Ensemble Learning. In: Ensemble Machine Learning. Springer, New York, New York, NY, pp. 1–34. https://doi.org/10.1007/978-1-4419-9326-7_1.
Prashanth, M., Kumar, A., Dhar, S., Verma, O., Rai, S.K., Kouser, B., 2023. Land use/land cover change and its implication on soil erosion in an ecologically sensitive Himachal Himalayan watershed, Northern India. Front. for. Glob. Chang. 6 https://doi.org/10.3389/ffgc.2023.1124677.
Qiu, X., Zhang, L., Nagaratnam Suganthan, P., Amaratunga, G.A.J., 2017. Oblique random forest ensemble via Least Square Estimation for time series forecasting. Inf. Sci. (ny) 420, 249–262. https://doi.org/10.1016/j.ins.2017.08.060.
Rajmohan, N., Prathapar, S.A., 2013. Hydrogeology of the Eastern Ganges Basin: an Overview. IWMI Working Papers. https://doi.org/10.5337/2013.216.
Rakotoarison, T.R., Hajalalaina, A.R., Raonivelo, A., Raherinirina, A., Zojaona, R.T., 2021. Spatial analysis of risks and vulnerabilities to major hazards in Madagascar using the multi-criteria method based on the analytical hierarchy process (AHP). J. Geosci. Environ. Prot. 09, 15–24. https://doi.org/10.4236/gep.2021.95003.
Rasyid, A.R., Bhandary, N.P., Yatabe, R., 2016. Performance of frequency ratio and logistic regression model in creating GIS based landslides susceptibility map at Lompobattang Mountain, Indonesia. Geoenviron. Disast. 3, 19. https://doi.org/10.1186/s40677-016-0053-x.
Roksandic, M., Dragicevic, S., Nenad, Ž., Kostadinov, S., Zlatic, M., 2011. Bank erosion as a factor of soil loss and land use changes in the Kolubara River Basin, Serbia. African J. Agric. Res. 6, 6604–6608. https://doi.org/10.5897/AJAR11.736.
Roshani, Rahaman, H., Rehman, Masroor, S., Sajjad, H., 2022a. Indicator-based inherent forest vulnerability using multicriteria decision-making analysis in the darjeeling district of West Bengal. In: Towards Sustainable Natural Resources. Springer International Publishing, Cham, pp. 51–67. https://doi.org/10.1007/978-3-031-06443-2_4.

Roshani, Sajjad, H., Saha, T.K., Rahaman, M.H., Masroor, M., Sharma, Y., Pal, S., 2022b. Analyzing trend and forecast of rainfall and temperature in Valmiki Tiger Reserve, India, using non-parametric test and random forest machine learning algorithm. Acta Geophysica 71, 531–552. https://doi.org/10.1007/s11600-022-00978-2.

Ross, D.S., Wemple, B.C., Willson, L.J., Balling, C.M., Underwood, K.L., Hamshaw, S.D., 2019. Impact of an extreme storm event on river corridor bank erosion and phosphorus mobilization in a mountainous watershed in the Northeastern United States. J. Geophys. Res. Biogeosciences 124, 18–32. https://doi.org/10.1029/2018JG004497.

Roy, P.S., Kushwaha, S.P.S., Murthy, M.S.R., Roy, A., Kushwah, D., Reddy, C.S., Behera, M.D., Mathur, V.B., Padalia, H., Saran, S., Singh, S., Jha, C.S., Porwal, M.C., 2012. Biodiversity Characterisation at Landscape level: National Assessment. Indian Institute of R I, 81–9014.

Roy, P.S., Behera, M.D., Murthy, M.S.R., Roy, A., Singh, S., Kushwaha, S.P.S., Jha, C.S., Sudhakar, S., Joshi, P.K., Reddy, C.S., Gupta, S., Pujar, G., Dutt, C.B.S., Srivastava, V. K., Porwal, M.C., Tripathi, P., Singh, J.S., Ramachandran, R.M., 2015. New vegetation type map of India prepared using satellite remote sensing: Comparison with global vegetation maps and utilities. International Journal of Applied Earth Observation and Geoinformation 39, 142–159. https://doi.org/10.1016/j.jag.2015.03.003.

Rusnák, M., Lehotský, M., Kidová, A., 2016. Channel migration inferred from aerial photographs, its timing and environmental consequences as responses to floods: A case study of the meandering Topľa River. Slovak Carpathians. Morav. Geogr. Reports 24, 32–43. https://doi.org/10.1515/mgr-2016-0015.

Saha, S., Sarkar, R., Roy, J., Saha, T.K., Bhardwaj, D., Acharya, S., 2022. Predicting the Landslide Susceptibility Using Ensembles of Bagging with RF and REPTree in Logchina, Bhutan. pp. 275–298. https://doi.org/10.1007/978-981-16-7314-6_12.

Saha, S., Gogoi, P., Gayen, A., Paul, G.C., 2021a. Constructing the machine learning techniques based spatial drought vulnerability index in Karnataka state of India. Journal of Cleaner Production 314, 128073. https://doi.org/10.1016/j.jclepro.2021.128073.

Saha, S., Kundu, B., Paul, G.C., Pradhan, B., 2023. Proposing an ensemble machine learning based drought vulnerability index using M5P, dagging, random sub-space and rotation forest models. Stoch. Environ. Res. Risk Assess. https://doi.org/10.1007/s00477-023-02403-6.

Saha, T.K., Pal, S., Talukdar, S., Debanshi, S., Khatun, R., Singha, P., Mandal, I., 2021b. How far spatial resolution affects the ensemble machine learning based flood susceptibility prediction in data sparse region. Journal of Environmental Management 297, 113344. https://doi.org/10.1016/j.jenvman.2021.113344.

Saikia, K., Goswami, T.K., 2020. Causes and consiquences of flood and bank erosion special reference to the middle Assam Brahmaputra Valley of Assam. J. Res. Humanit. Soc. Sci. 8, 01–05.

Saikia, L., Mahanta, C., Mukherjee, A., Borah, S.B., 2019. Erosion–deposition and land use/land cover of the Brahmaputra river in Assam, India. J. Earth Syst. Sci. 128, 211. https://doi.org/10.1007/s12040-019-1233-3.

Sarkar, A., 2017. Brahmaputra River Bank Failures—Causes and Impact on River Dynamics. In: Advancing Culture of Living with Landslides. Springer International Publishing, Cham, pp. 273–280. https://doi.org/10.1007/978-3-319-53483-1_32.

Sarkar, A., Garg, R.D., Sharma, N., 2012. RS-GIS, after the 2004 tsunami. Marine Geodesy 38 (1), 26–39. https://doi.org/10.1080/01490419.2014.908795.

Sarma, J.N., 2005. Fluvial process and morphology of the Brahmaputra River in Assam, India. Geomorphology 70, 226–256. https://doi.org/10.1016/j.geomorph.2005.02.007.

Sarma, A., 2014. Landscape Degradation of River Island Majuli, Assam (India) due to Flood and Erosion by River Brahmaputra and Its Restoration. J. Med. Bioeng. 272–276. https://doi.org/10.12720/jomb.3.4.272-276.

Sarma, J., Phukan, M., 2006. Bank erosion and bankline migration of the Brahmaputra River in Assam during the twentieth century. Journal of the Geological Society of India 68, 1023–1036.

Sharma, N., Amoako Johnson, F., Hutton, W.C., Clark, M., 2010. Hazard, vulnerability and risk on the Brahmaputra basin: a case study of river bank erosion. The Open Hydrology Journal 4 (1).

Shichkin, A.V., Buevich, A.G., Sergeev, A.P., 2018. Comparison of artificial neural network, random forest and random perceptron forest for forecasting the spatial impurity distribution. In: AIP Conference Proceedings, Vol. 1982, No. 1. AIP Publishing, p. 020005. https://doi.org/10.1063/1.5045411.

Simmons, E.A., 2004. Landscape and Planning | Landscape Ecology, the Concepts, in: Encyclopedia of Forest Sciences. Elsevier, pp. 502–508, https://doi.org/10.1016/B0-12-145160-7/00022-3.

Singh, S., 2008. Erosion and Weathering in the Brahmaputra River System. pp. 373–393, https://doi.org/10.1002/9780470723722.ch18.

Singha, P., Das, P., Talukdar, S., Pal, S., 2020. Modeling livelihood vulnerability in erosion and flooding induced river island in Ganges riparian corridor, India. Ecological Indicators 119, 106825. https://doi.org/10.1016/j.ecolind.2020.106825.

Szczyrba, L., Zhang, Y., Pamukcu, D., Eroglu, D.I., Weiss, R., 2021. Quantifying the role of vulnerability in hurricane damage via a machine learning case study. Nat. Hazards Rev. 22 https://doi.org/10.1061/(ASCE)NH.1527-6996.0000460.

Talukdar, S., Pal, S., Chakraborty, A., Mahato, S., 2020. Damming effects on trophic and habitat state of riparian wetlands and their spatial relationship. Ecological Indicators 118, 106757. https://doi.org/10.1016/j.ecolind.2020.106757.

Talukdar, S., Pal, S., Singha, P., 2021. Proposing artificial intelligence based livelihood vulnerability index in river islands. Journal of Cleaner Production 284, 124707. https://doi.org/10.1016/j.jclepro.2020.124707.

Tempa, K., 2022. District flood vulnerability assessment using analytic hierarchy process (AHP) with historical flood events in Bhutan. PLoS One 17, e0270467. https://doi.org/10.1371/journal.pone.0270467.

USGS, 2018. NDVI, the Foundation for Remote Sensing Phenology. https://www.usgs.gov/special-topics/remote-sensing-phenology/science/ndvi-foundation-remote-sensing. (accessed 01 August 2023).

Walz, Y., Janzen, S., Narvaez, L., Ortiz-Vargas, A., Woelki, J., Doswald, N., Sebesvari, Z., 2021. Disaster-related losses of ecosystems and their services. Why and how do losses matter for disaster risk reduction? International Journal of Disaster Risk Reduction 63, 102425. https://doi.org/10.1016/j.ijdrr.2021.102425.

Water Resources. Flood and Erosion Problems. Gov. Assam. URL https://waterresources.assam.gov.in/portlets/flood-erosion-problems (Last accessed 17/03/23).

Wu, J., 2019. Landscape Ecology. In: Encyclopedia of Ecology. Elsevier, pp. 527–531. https://doi.org/10.1016/B978-0-12-409548-9.10919-4.

Yan, J., Li, G., Wang, H., Zhang, M., Sun, D., Kang, X., 2021. Landscape ecological risk assessment and spatiotemporal change analysis in Yonghe County. E3S Web Conf. 237, 04038. https://doi.org/10.1051/e3sconf/202123704038.

Yu, H., Zhang, X., Deng, Y., 2022. Spatiotemporal evolution and influencing factors of landscape ecological vulnerability in the three-river-source national park region. Chinese Geogr. Sci. 32, 852–866. https://doi.org/10.1007/s11769-022-1297-x.

Yusoff, N., Abidin, R.J., 2023. River bank erosion risk with regards to rainfall erosivity. Infrastruct. Univ. Kuala Lumpur Res. J. 1, 1.

Zhang, X., Shi, P., Luo, J., 2013. Landscape ecological risk assessment of the Shiyang River basin. In: Geo-Informatics in Resource Management and Sustainable Ecosystem: International Symposium, GRMSE 2013, Wuhan, China, November 8-10, 2013, Proceedings, Part II 1. Springer, Berlin Heidelberg, pp. 98–106. https://doi.org/10.1007/978-3-642-41908-9_10.